

Supporting Information

Table S1. Selected bond lengths (\AA) and angles ($^\circ$) for **1**

V1—O1	1.619 (3)	V2—O6	1.625 (3)	V3—O5	1.621 (3)
V1—O10	2.009 (3)	V2—O10	2.018 (3)	V3—O11	2.025 (3)
V1—O13	2.133 (3)	V2—O13	2.017 (3)	V3—O13	1.870 (3)
V1—O19	1.971 (3)	V2—O14	1.888 (3)	V3—O14	2.020 (3)
V1—N1	2.134 (4)	V2—O16	2.384 (3)	V3—O15	2.422 (3)
V1—N2	2.149 (4)	V2—O18	1.724 (3)	V3—O20	1.742 (3)
V4—O3	1.614 (3)	V5—O4	1.617 (3)	V6—O7	1.629 (3)
V4—O11	1.999 (3)	V5—O9	2.001 (3)	V6—O9	2.030 (3)
V4—O14	2.110 (3)	V5—O16	2.099 (3)	V6—O14	2.393 (3)
V4—O17	1.973 (3)	V5—O18	1.961 (3)	V6—O15	1.849 (3)
V4—N3	2.149 (4)	V5—N5	2.121 (4)	V6—O16	1.991 (3)
V4—N4	2.124 (4)	V5—N6	2.152 (4)	V6—O17	1.748 (3)
V7—O8	1.618 (3)	V7—O16	1.898 (3)	V8—O15	2.148 (3)
V7—O12	2.005 (3)	V7—O19	1.724 (3)	V8—O20	1.979 (3)
V7—O13	2.406 (3)	V8—O2	1.602 (3)	V8—N7	2.149 (4)
V7—O15	2.045 (3)	V8—O12	2.009 (3)	V8—N8	2.128 (4)
O1—V1—O10	102.45 (13)	O6—V2—O10	94.63 (13)	O5—V3—O11	95.33 (13)
O1—V1—O13	176.23 (13)	O6—V2—O13	104.87 (14)	O5—V3—O13	100.65 (14)
O1—V1—O19	102.96 (14)	O6—V2—O14	99.82 (14)	O5—V3—O14	104.23 (14)
O1—V1—N1	98.35 (14)	O6—V2—O16	176.71 (13)	O5—V3—O15	177.32 (13)
O1—V1—N2	96.05 (15)	O6—V2—O18	104.34 (15)	O5—V3—O20	104.99 (15)
O10—V1—O13	74.59 (11)	O10—V2—O16	88.39 (10)	O11—V3—O15	86.85 (11)
O10—V1—N1	158.47 (13)	O13—V2—O10	77.00 (11)	O13—V3—O11	153.87 (12)
O10—V1—N2	92.61 (13)	O13—V2—O16	74.52 (11)	O13—V3—O14	79.26 (12)
O13—V1—N1	84.39 (12)	O14—V2—O10	154.41 (12)	O13—V3—O15	76.76 (11)
O13—V1—N2	81.86 (12)	O14—V2—O13	78.92 (11)	O14—V3—O11	76.84 (11)

O19—V1—O10	88.31 (12)	O14—V2—O16	76.89 (11)	O14—V3—O15	74.71 (10)
O19—V1—O13	79.43 (11)	O18—V2—O10	93.71 (13)	O20—V3—O11	92.73 (12)
O19—V1—N1	92.43 (12)	O18—V2—O13	149.94 (13)	O20—V3—O13	102.81 (13)
O19—V1—N2	160.31 (13)	O18—V2—O14	102.92 (13)	O20—V3—O14	149.72 (13)
N1—V1—N2	79.64 (13)	O18—V2—O16	76.72 (12)	O20—V3—O15	76.42 (12)
O3—V4—O11	101.93 (14)	O4—V5—O9	101.39 (14)	O7—V6—O9	94.12 (14)
O3—V4—O14	176.71 (15)	O4—V5—O16	174.93 (14)	O7—V6—O14	179.26 (13)
O3—V4—O17	102.41 (15)	O4—V5—O18	103.67 (14)	O7—V6—O15	101.02 (14)
O3—V4—N3	94.67 (16)	O4—V5—N5	97.18 (16)	O7—V6—O16	104.58 (13)
O3—V4—N4	97.15 (15)	O4—V5—N6	94.43 (16)	O7—V6—O17	104.11 (14)
O11—V4—O14	75.36 (11)	O9—V5—O16	74.73 (11)	O9—V6—O14	86.27 (11)
O11—V4—N3	93.79 (13)	O9—V5—N5	160.65 (14)	O15—V6—O9	155.03 (12)
O11—V4—N4	160.40 (13)	O9—V5—N6	93.06 (13)	O15—V6—O14	78.39 (11)
O14—V4—N3	83.71 (13)	O16—V5—N5	86.42 (13)	O15—V6—O16	80.54 (12)
O14—V4—N4	85.42 (12)	O16—V5—N6	82.64 (13)	O16—V6—O9	76.48 (11)
O17—V4—O11	88.48 (12)	O18—V5—O9	87.95 (12)	O16—V6—O14	74.90 (10)
O17—V4—O14	79.52 (11)	O18—V5—O16	79.63 (11)	O17—V6—O9	91.79 (13)
O17—V4—N3	161.93 (13)	O18—V5—N5	92.96 (13)	O17—V6—O14	76.50 (12)
O17—V4—N4	91.84 (13)	O18—V5—N6	161.31 (13)	O17—V6—O15	103.45 (13)
N4—V4—N3	80.09 (14)	N5—V5—N6	80.03 (14)	O17—V6—O16	149.65 (13)
O8—V7—O12	96.36 (14)	O16—V7—O15	78.03 (11)	O12—V8—O15	74.01 (11)
O8—V7—O13	175.42 (13)	O19—V7—O12	94.25 (12)	O12—V8—N7	92.29 (13)
O8—V7—O15	104.71 (13)	O19—V7—O13	76.99 (12)	O12—V8—N8	159.45 (14)
O8—V7—O16	99.41 (14)	O19—V7—O15	149.96 (13)	O15—V8—N7	81.19 (13)
O8—V7—O19	104.67 (15)	O19—V7—O16	103.14 (13)	O20—V8—O12	88.82 (12)
O12—V7—O13	87.73 (11)	O2—V8—O12	100.54 (14)	O20—V8—O15	79.07 (11)
O12—V7—O15	76.40 (11)	O2—V8—O15	174.17 (15)	O20—V8—N7	159.11 (13)
O15—V7—O13	74.20 (10)	O2—V8—O20	103.16 (15)	O20—V8—N8	91.66 (13)
O16—V7—O12	152.63 (12)	O2—V8—N7	97.15 (15)	N8—V8—O15	85.91 (13)

O16—V7—O13 76.03 (11) O2—V8—N8 99.36 (16) N8—V8—N7 80.13 (14)

The space-filling plot of the $[V_8O_{12}(OH)_4(CH_3O)_4(DAC)_4]$ unit with a diameter of about 1.6 nm is revealed in Figure 1g. The adjacent V_8 units are expanded each other through H-bond between the V_8 units and the lattice methanol molecules with the nearest distance of 11.999 (1) Å. The nearest $V \cdots V$ distance between the adjacent V_8 units is 5.2172 (5) Å, indicating the presence of weak magnetic exchange interaction between them. (Figure S1)

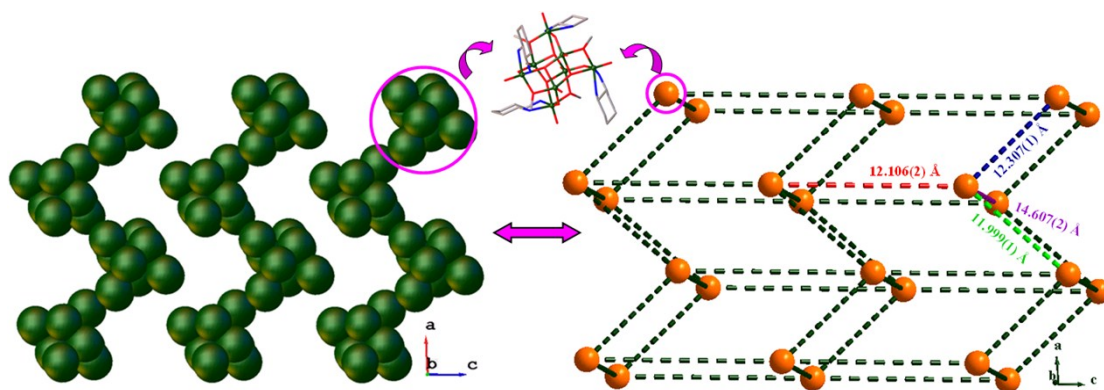


Figure S1 Packing of the V_8 clusters within the crystallographic ac plane.

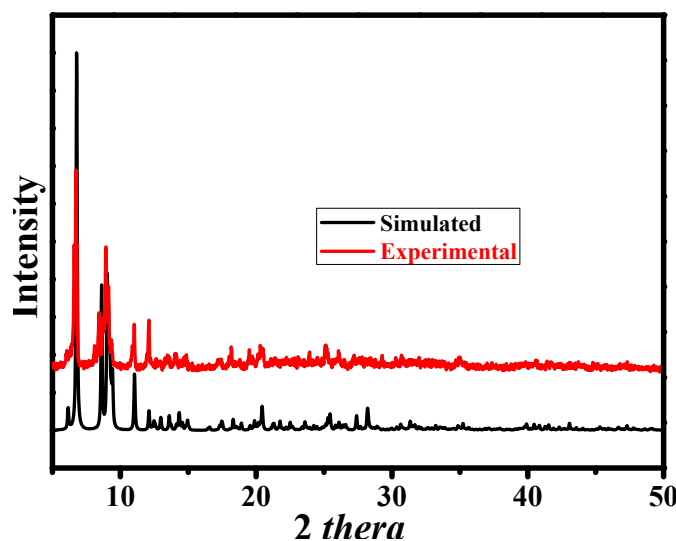


Figure S2 Measured and calculated powder X-ray diffraction (PXRD) pattern of **1**.

Magnetic Properties

Magnetic susceptibility measurement was carried out on polycrystalline sample of **1** in the temperature range 2.0-300.0 K at 1000 Oe. (Figure S3a) The data above 2 K follow the Curie-Weiss law with $C = 3.12 \text{ cm}^3 \cdot \text{K} \cdot \text{mol}^{-1}$ and $\theta = -13.05 \text{ K}$. The $\chi_M T$ value at 300 K is $2.98 \text{ cm}^3 \cdot \text{K} \cdot \text{mol}^{-1}$, which is in accord with the spin-only value $3 \text{ cm}^3 \cdot \text{K} \cdot \text{mol}^{-1}$ for eight magnetically active V(IV) ions ($S = 1/2$, $g = 2.0$). As the temperature is lowered, the $\chi_M T$ values decrease continuously and reaches a local minimum of $0.34 \text{ cm}^3 \cdot \text{K} \cdot \text{mol}^{-1}$ at about 2 K, indicative of a weak antiferromagnetic interaction. The in- and out-of-phase ac susceptibilities have no dependence on frequency between 2 and 10 K for **1** indicating that there is no single-molecule magnet (SMM) behavior in **1** (Figure S3b). We also investigated the variation of the magnetization M with the applied magnetic field H for **1** in the range of 0-50 kOe at 2 K (Figure S3c). The magnetization increase nearly linearly to $0.96 \text{ N}\beta$ at 50KOe, far from the saturation sum values of eight V(IV) ions. And no obvious hysteresis loops are observed for **1**.

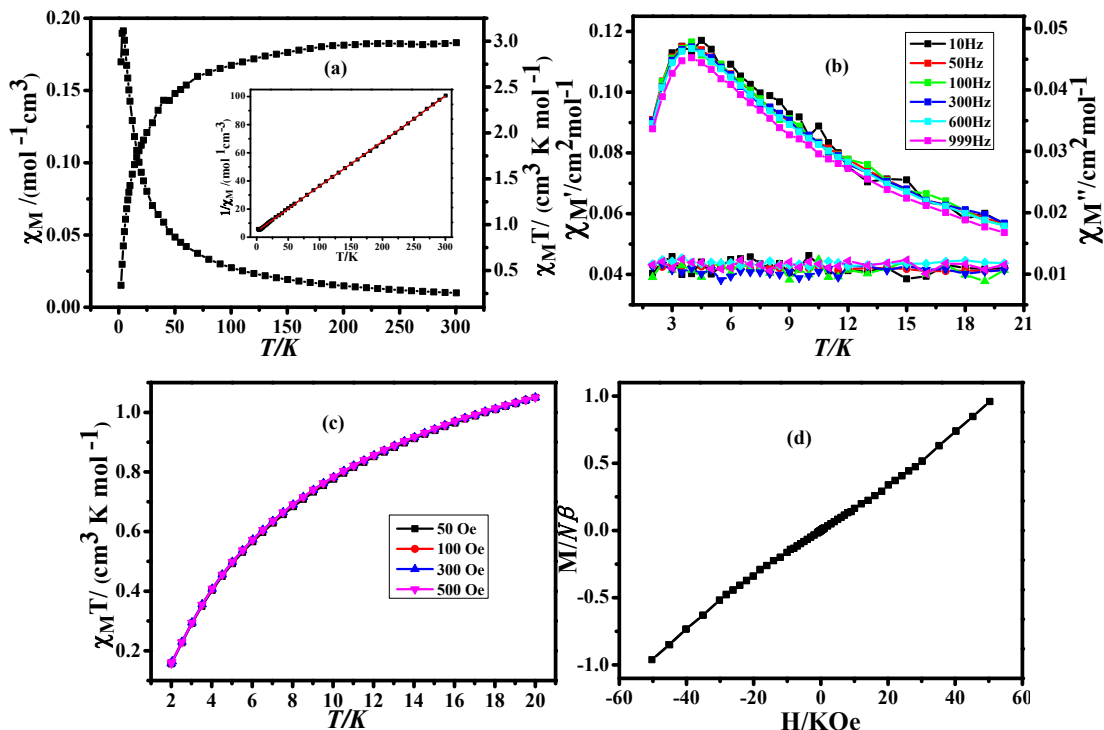


Figure S3 (a) Plots of $\chi_M T$ vs T, χ_M vs T and χ_M^{-1} vs T (inset) for **1**; (b) the zero-field ac magnetic susceptibilities from 2- 10 K for **1**; (c) FC magnetization of them in different field; (d) field dependency of magnetization of **1** at 2 K.

Thermal Analyses

The thermogravimetric (TG) analysis was performed in N₂ atmosphere on polycrystalline sample of complex **1**, and the TG curve is shown in Figure S4. The first weight loss of 15.15% between 35 and 102 °C corresponds to the release of the lattice methanol molecules (calculated, 15.27%). The residual framework decomposed beyond 371 °C in a series of complicated weight losses until 532 °C.

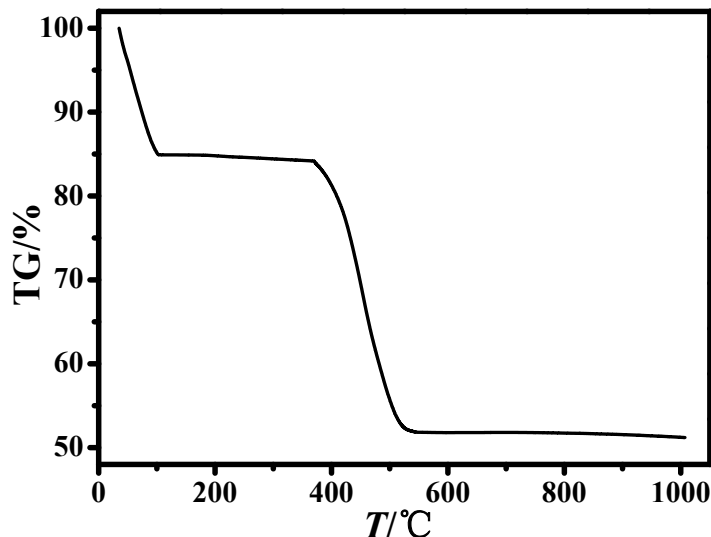
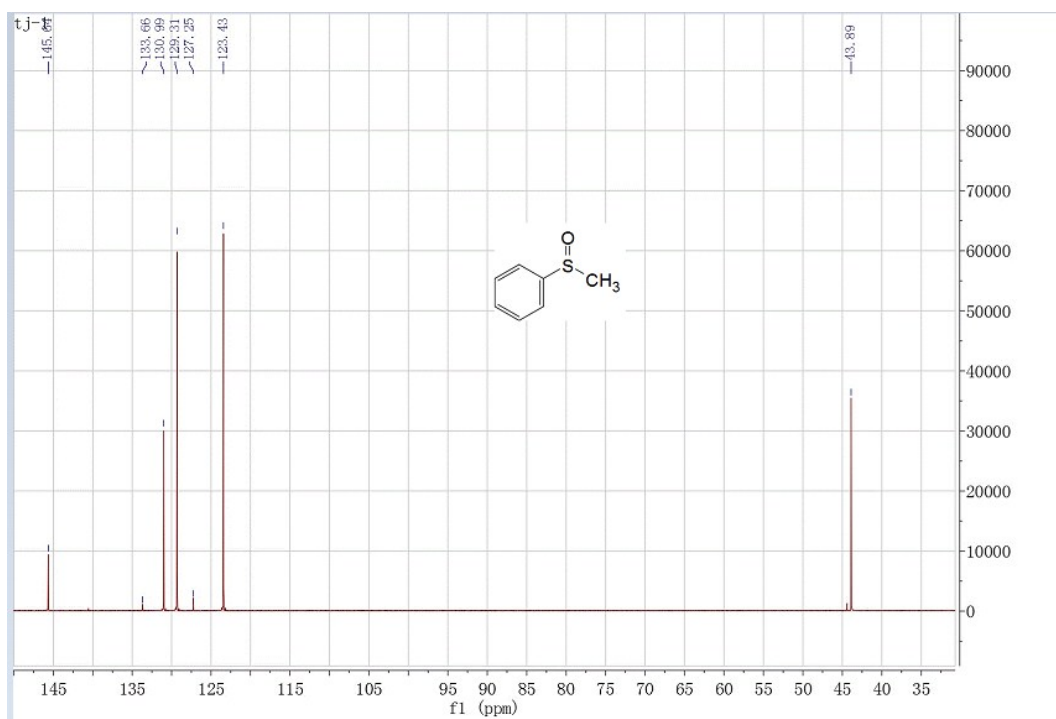
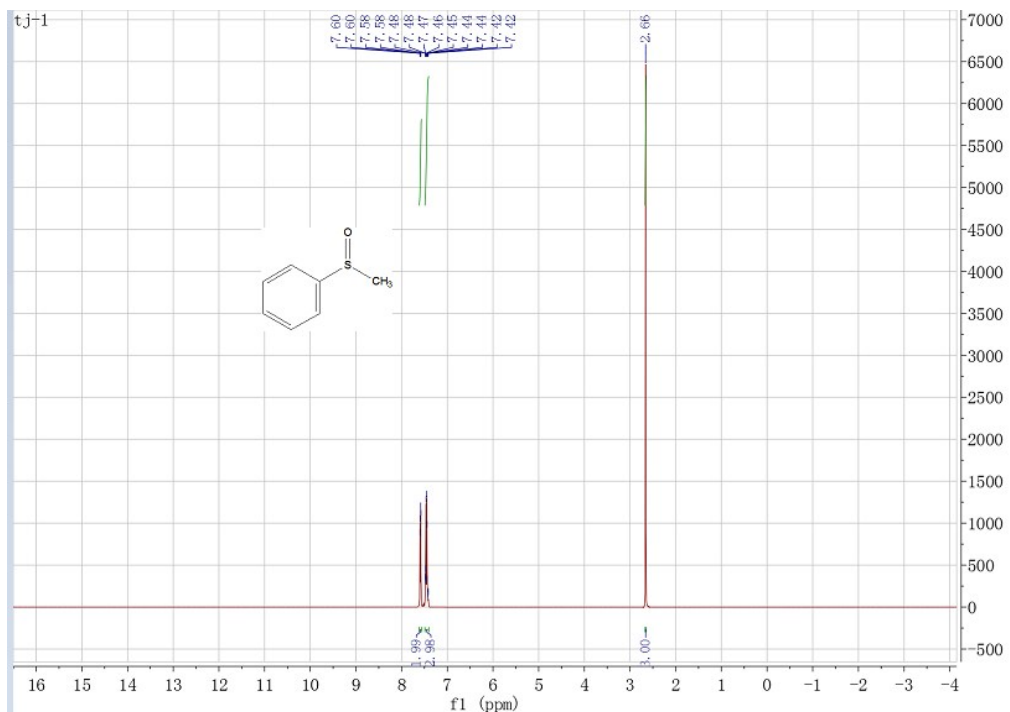


Figure S4 TGA curve for complexes **1**.

¹H NMR and ¹³C NMR of sulfoxides:

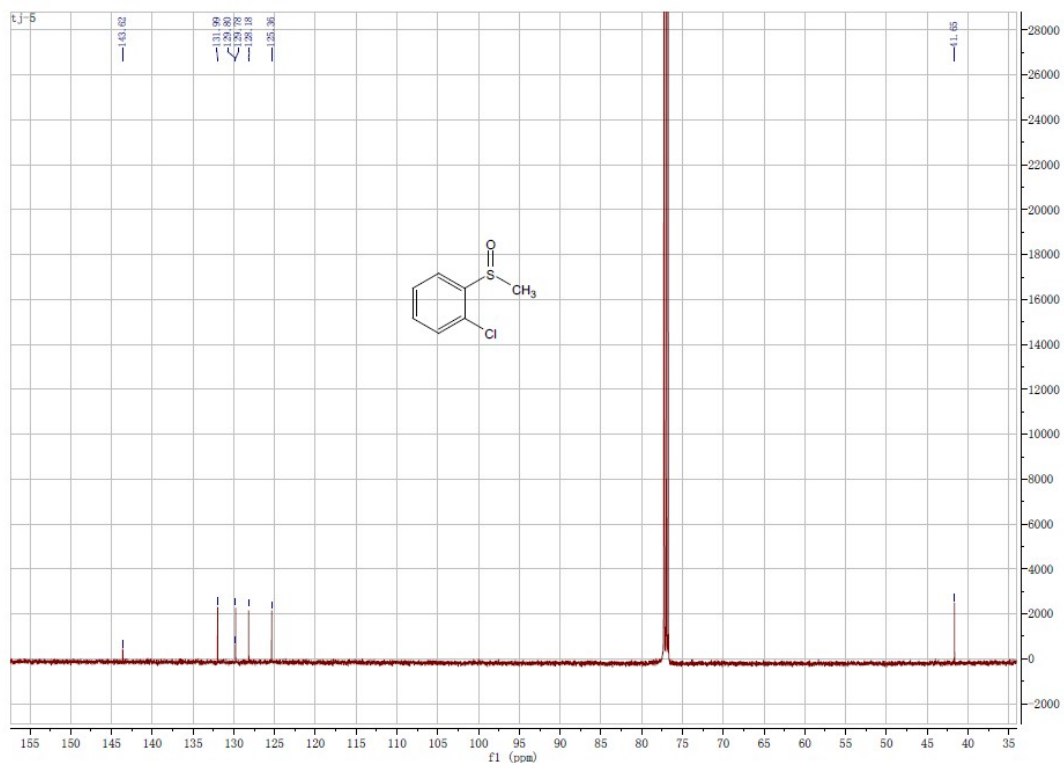
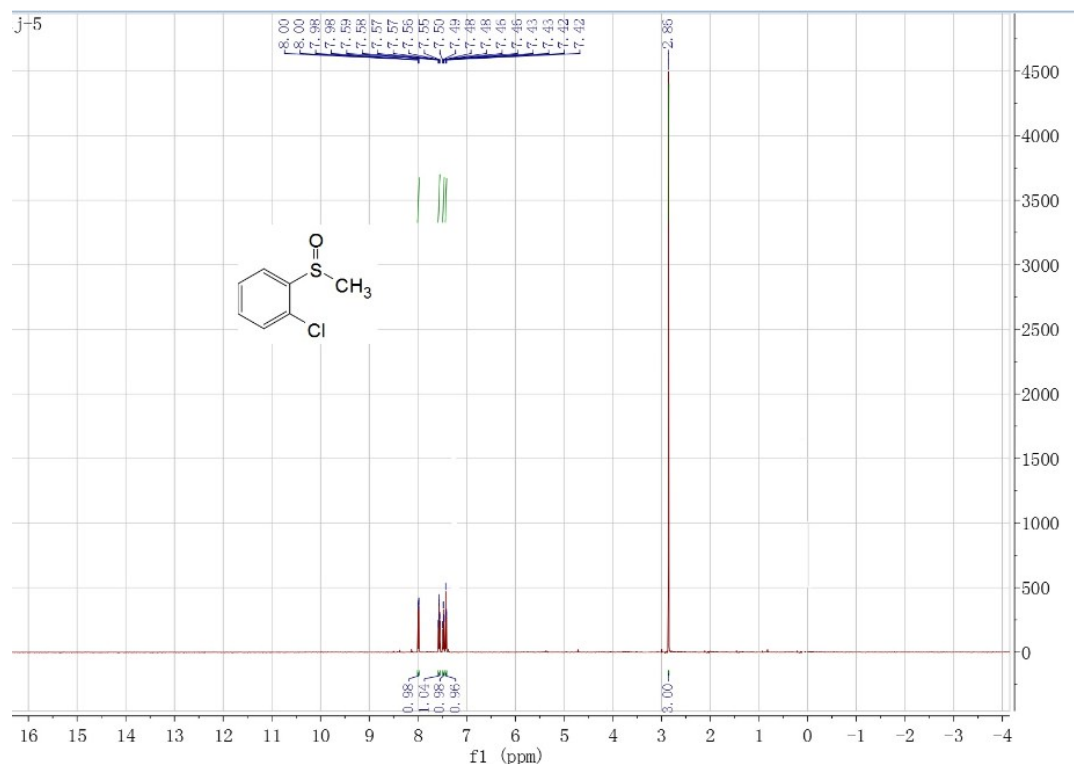
Methyl phenyl sulfoxide. Yellow oil, purified by flash chromatography on silica gel (ethyl acetate/petroleum ether, v/v = 3:1) (89%). ¹H NMR (500 MHz, CDCl₃) δ (ppm): 7.59 (dd, *J* = 7.90, 1.4 Hz, 2H), 7.49-7.41 (m, 3H), 2.66 (s, 3H); ¹³C NMR (126 MHz, CDCl₃) δ (ppm): 145.6, 133.7, 131.0, 129.3, 127.3, 123.4, 43.9. Determination of *ee*

by HPLC analysis: *n*-hexane/2-PrOH (80:20), 0.8 mL/min, 254 nm, $t_r(S) = 14.0$ min, $t_r(R) = 24.0$ min.

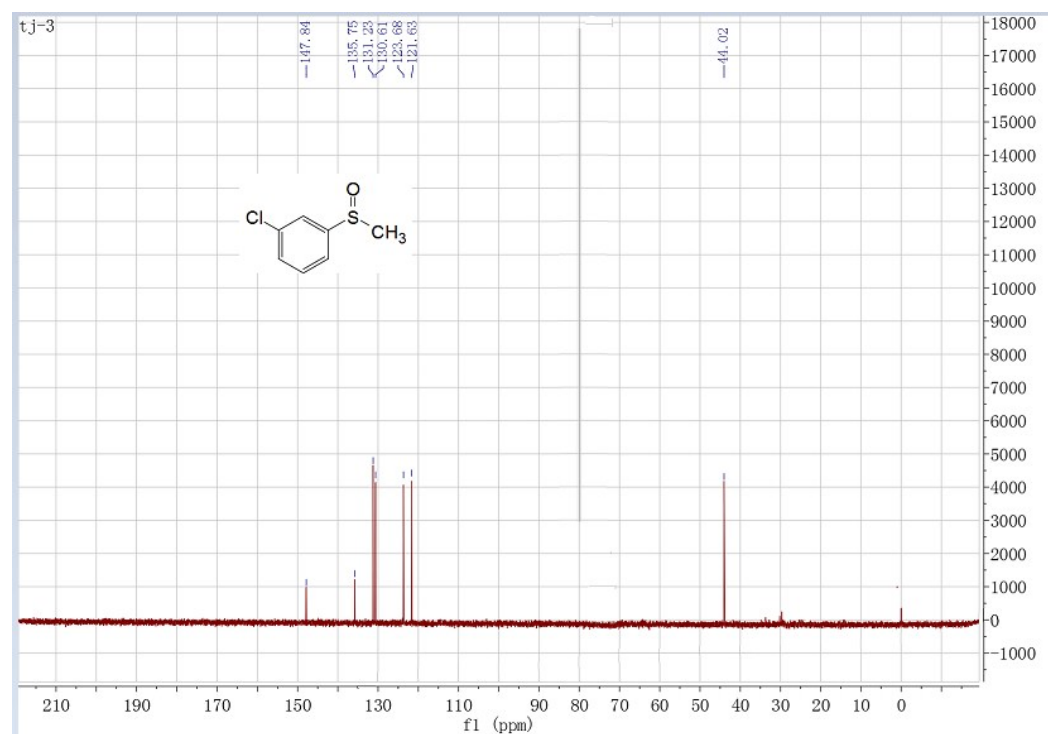
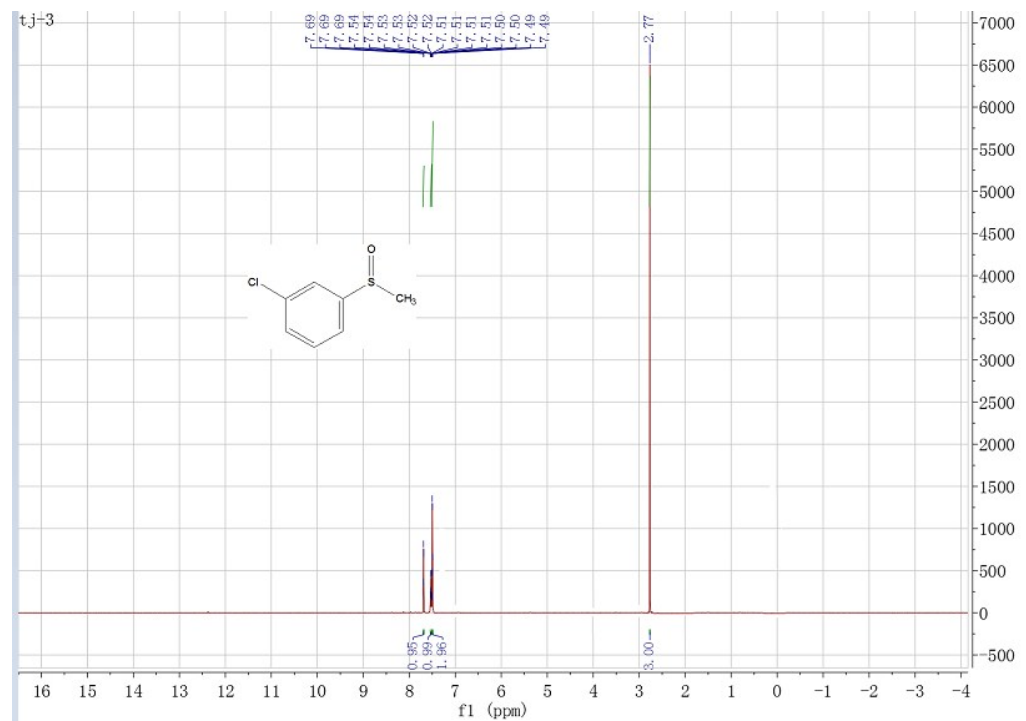


2-Chlorophenyl methyl sulfoxide. Colorless oil, purified by flash chromatography on silica gel (ethyl acetate/petroleum ether, v/v = 2:3) (29%). ^1H NMR (500 MHz, CDCl_3) δ (ppm): 7.99 (dd, J = 7.8, 1.6 Hz, 1H), 7.57 (td, J = 7.7, 1.2 Hz, 1H), 7.48 (td,

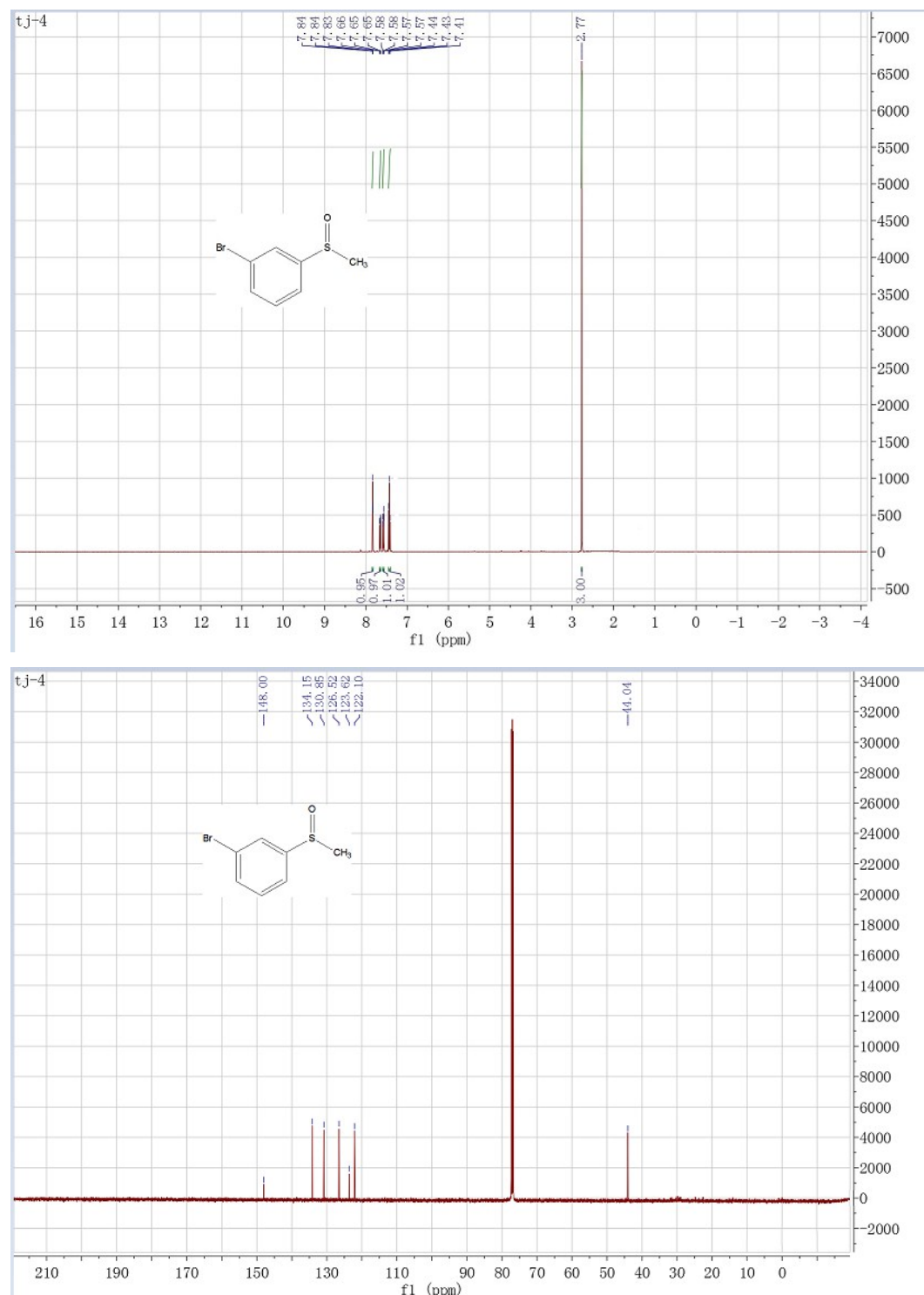
$J = 7.6, 1.6$ Hz, 1H), 7.43 (dd, $J = 7.9, 1.1$ Hz, 1H), 2.86 (s, 3H); ^{13}C NMR (126 MHz, CDCl_3) δ (ppm): 143.6, 132.0, 129.8, 129.8, 128.2, 125.4, 41.7. Determination of *ee* by HPLC analysis: *n*-hexane/2-PrOH (90:10), 1 mL/min, 254 nm, t_r (*S*) = 11.3 min, t_r (*R*) = 22.0 min.



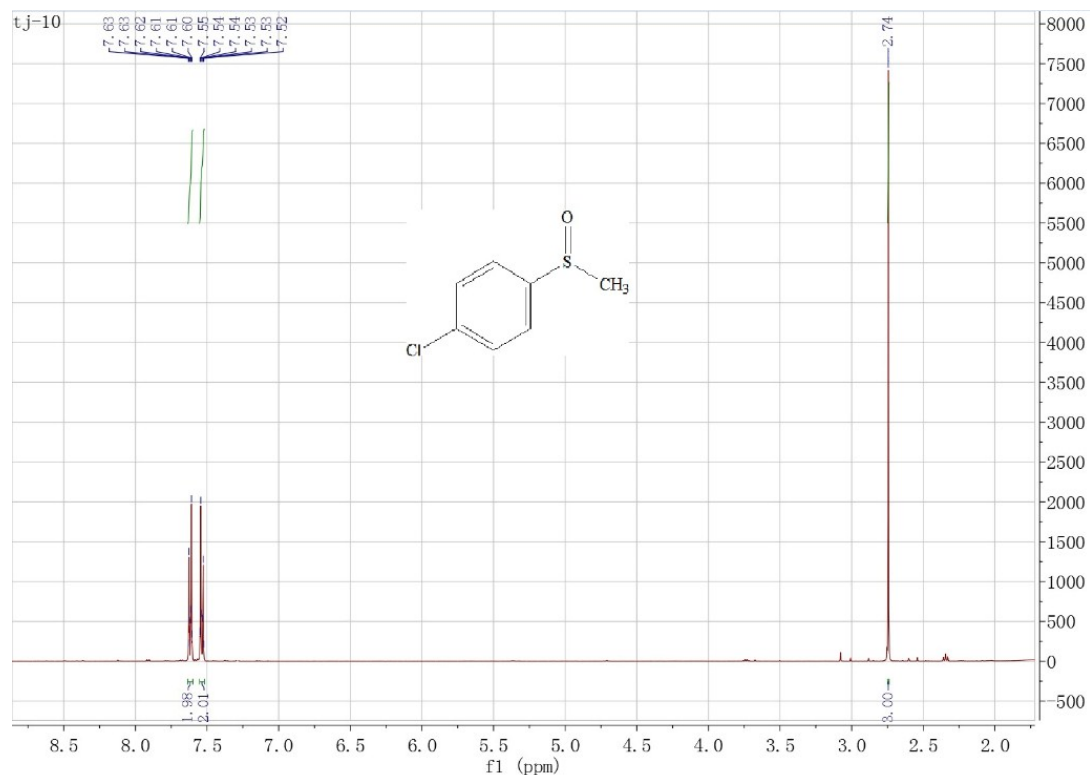
3-Chlorophenyl methyl sulfoxide. Colorless oil, purified by flash chromatography on silica gel (ethyl acetate/petroleum ether, $v/v = 2:3$) (40%). ^1H NMR (500 MHz, CDCl_3) δ (ppm): 7.69 (t, $J = 1.1$ Hz, 1H), 7.53 (qd, $J = 3.8, 1.3$ Hz, 1H), 7.50 (td, $J = 4.3, 2.0$ Hz, 2H), 2.77 (s, 3H); ^{13}C NMR (126 MHz, CDCl_3) δ (ppm): 147.9, 135.8, 131.2, 130.6, 123.7, 121.6, 44.0. Determination of *ee* by HPLC analysis: *n*-hexane/2-PrOH (90:10), 1 mL/min, 254 nm, t_r (*S*) = 15.0 min, t_r (*R*) = 21.5 min.

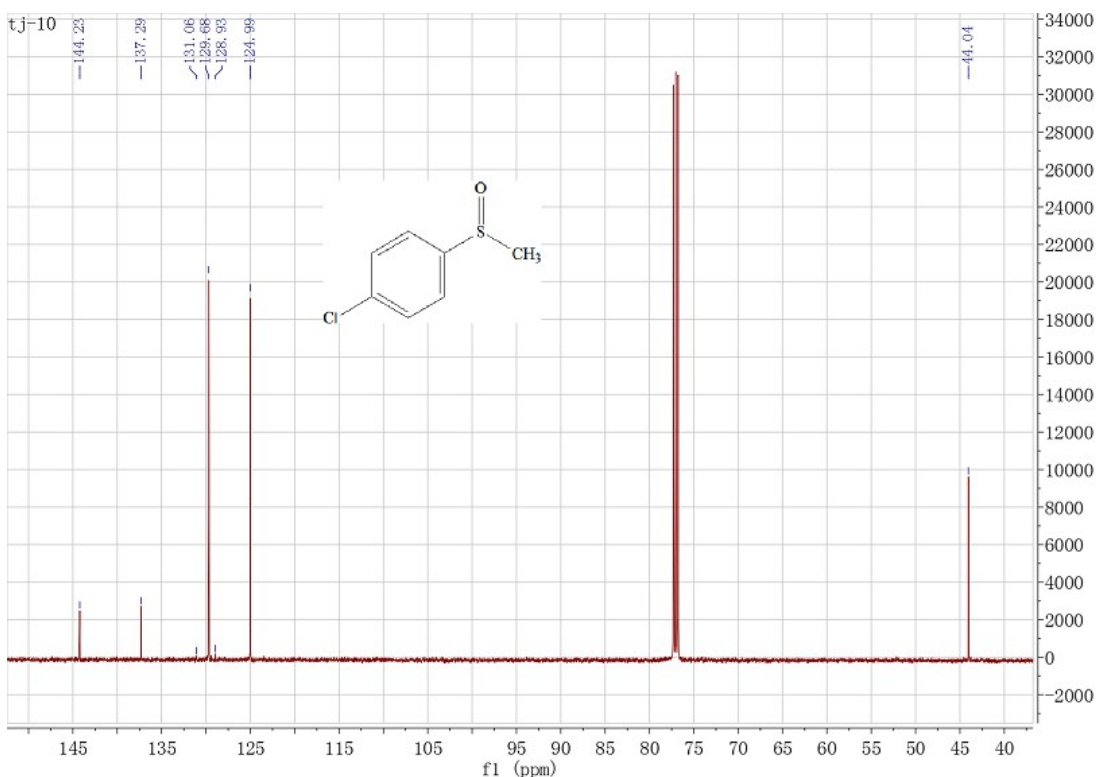


3-Bromophenyl methyl sulfoxide. Colorless oil, purified by flash chromatography on silica gel (ethyl acetate/petroleum ether, $v/v = 2:3$) (46%). ^1H NMR (500 MHz, CDCl_3) δ (ppm): 7.84 (t, $J = 1.7$ Hz, 1H), 7.67-7.64 (m, 1H), 7.58 (dd, $J = 7.8, 1.1$ Hz, 1H), 7.43 (t, $J = 7.9$ Hz, 1H), 2.77 (s, 3H); ^{13}C NMR (126 MHz, CDCl_3) δ (ppm): 148.0, 134.2, 130.9, 126.5, 123.6, 122.0, 44.0. Determination of *ee* by HPLC analysis: *n*-hexane/2-PrOH (80:20), 1 mL/min, 254 nm, t_r (*S*) = 10.7 min, t_r (*R*) = 16.1 min.

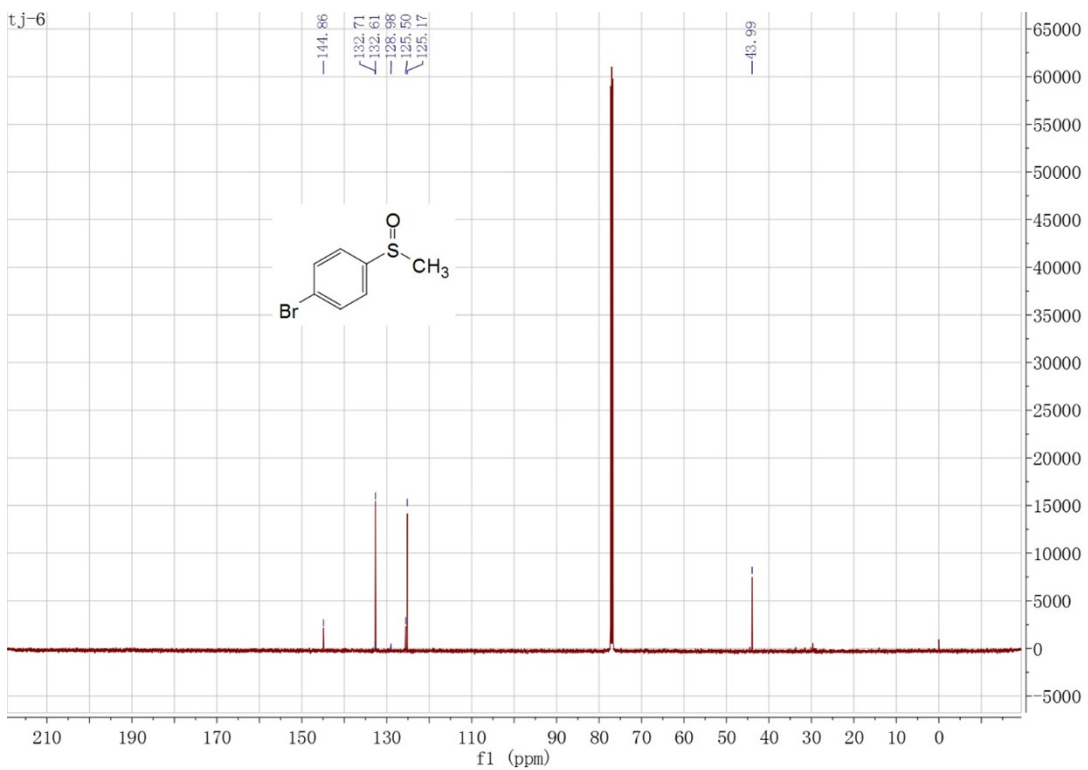
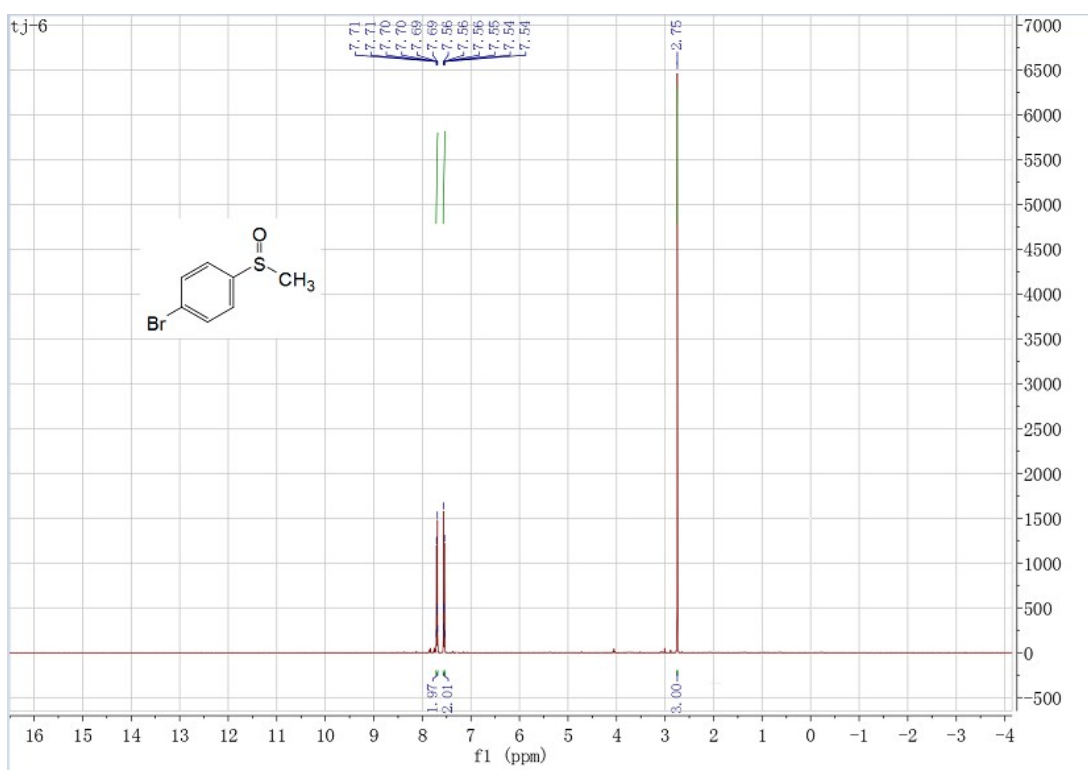


4-Chlorophenyl methyl sulfoxide. Colorless oil, purified by flash chromatography on silica gel (ethyl acetate/petroleum ether, $v/v = 2:3$) (63%). ^1H NMR (500 MHz, CDCl_3) δ (ppm): 7.63-7.60 (m, 2H), 7.55-7.52 (m, 2H), 2.74 (s, 3H); ^{13}C NMR (126 MHz, CDCl_3) δ (ppm): 144.2, 137.3, 131.1, 129.7, 128.9, 125.0, 44.0. Determination of *ee* by HPLC analysis: *n*-hexane/2-PrOH (90:10), 1 mL/min, 254 nm, t_r (*S*) = 14.2 min, t_r (*R*) = 23.7 min.



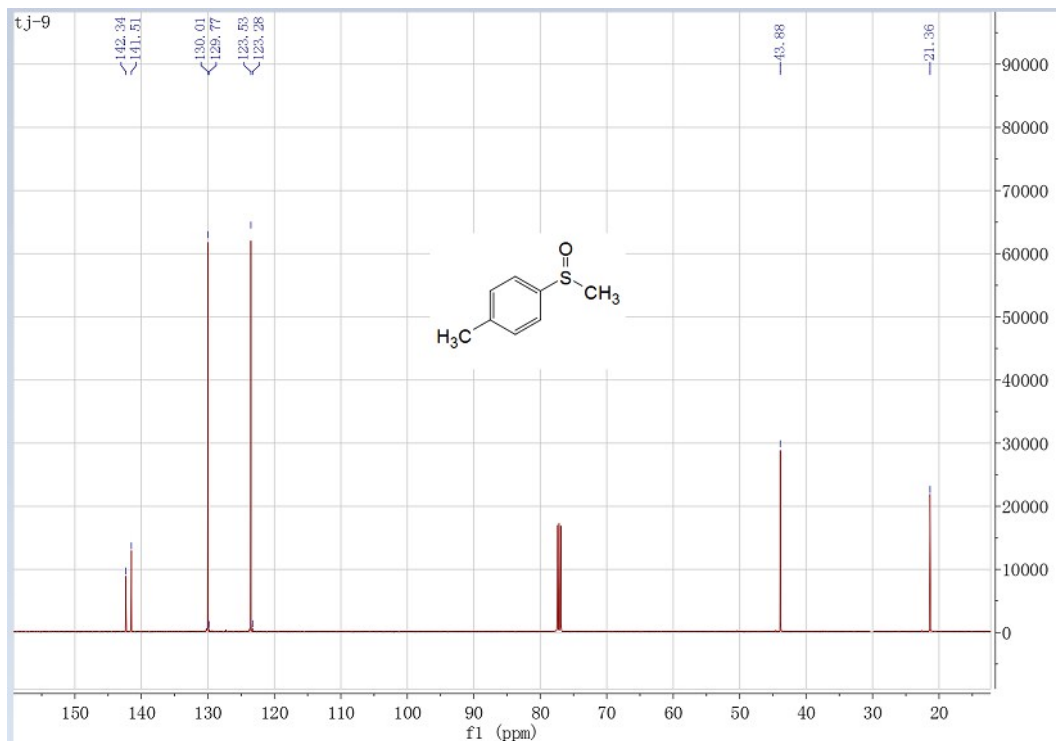
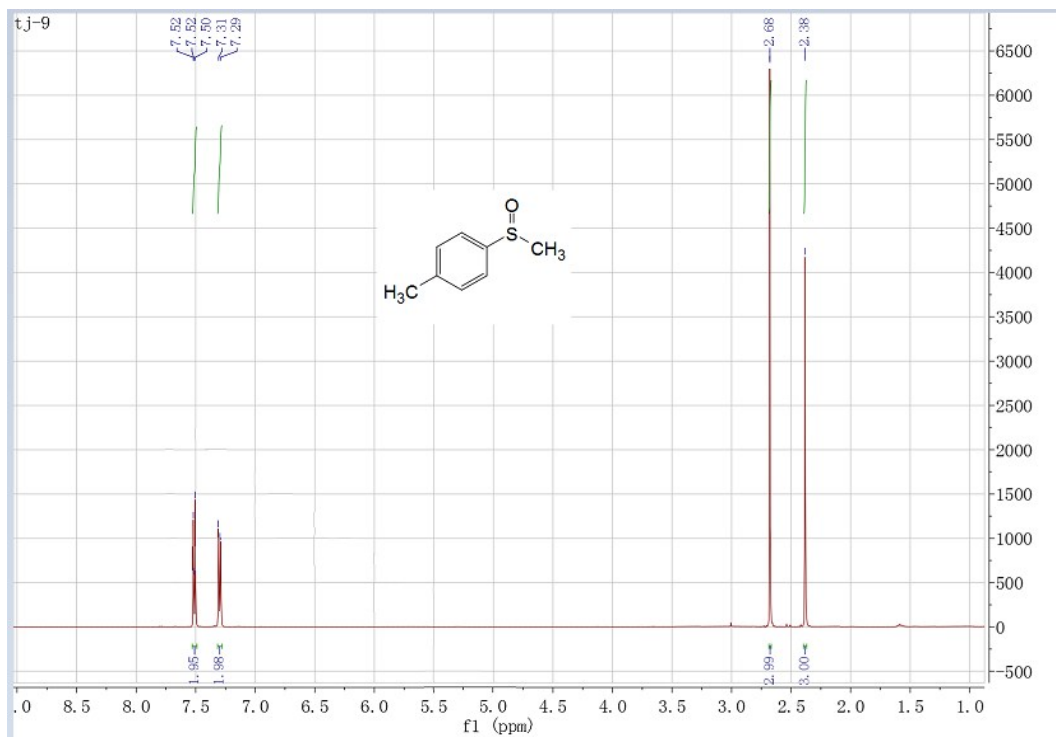


4-Bromophenyl methyl sulfoxide. Colorless oil, purified by flash chromatography on silica gel (ethyl acetate/petroleum ether, $v/v = 2:3$) (44%). ^1H NMR (500 MHz, CDCl_3) δ (ppm): 7.72-7.68 (m, 2H), 7.57-7.53 (m, 2H), 2.75 (s, 3H); ^{13}C NMR(126 MHz, CDCl_3) δ (ppm): 144.9, 132.7, 132.6, 129.0, 125.5, 125.2, 44.0. Determination of *ee* by HPLC analysis: *n*-hexane/2-PrOH (80:20), 0.8 mL/min, 254 nm, t_r (*S*) = 12.2 min, t_r (*R*) = 17.7 min.



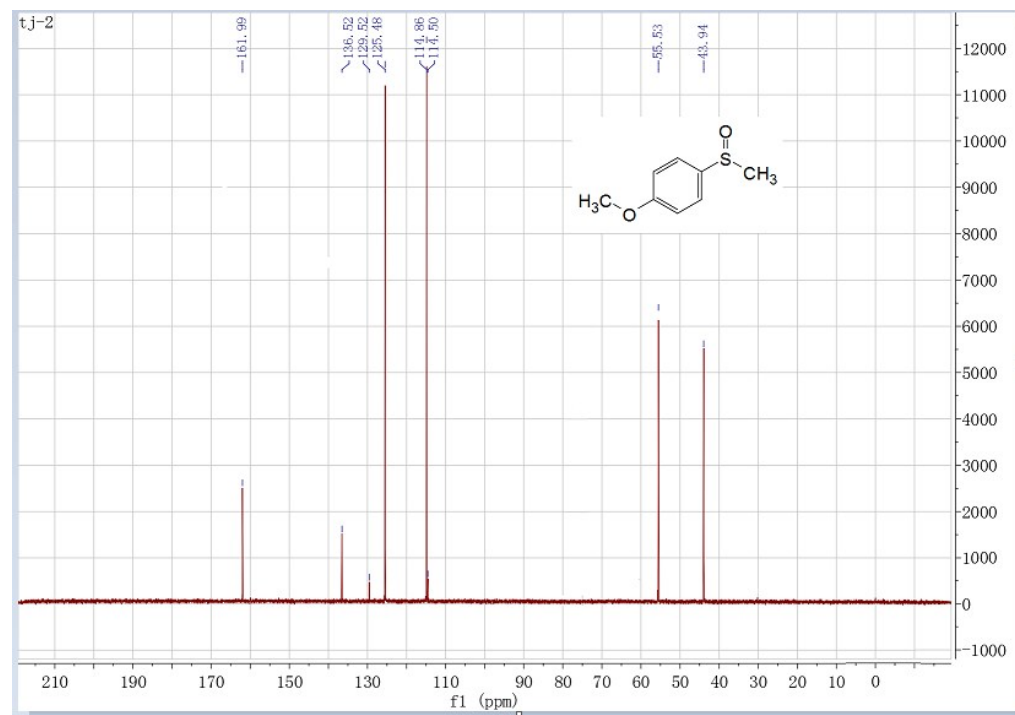
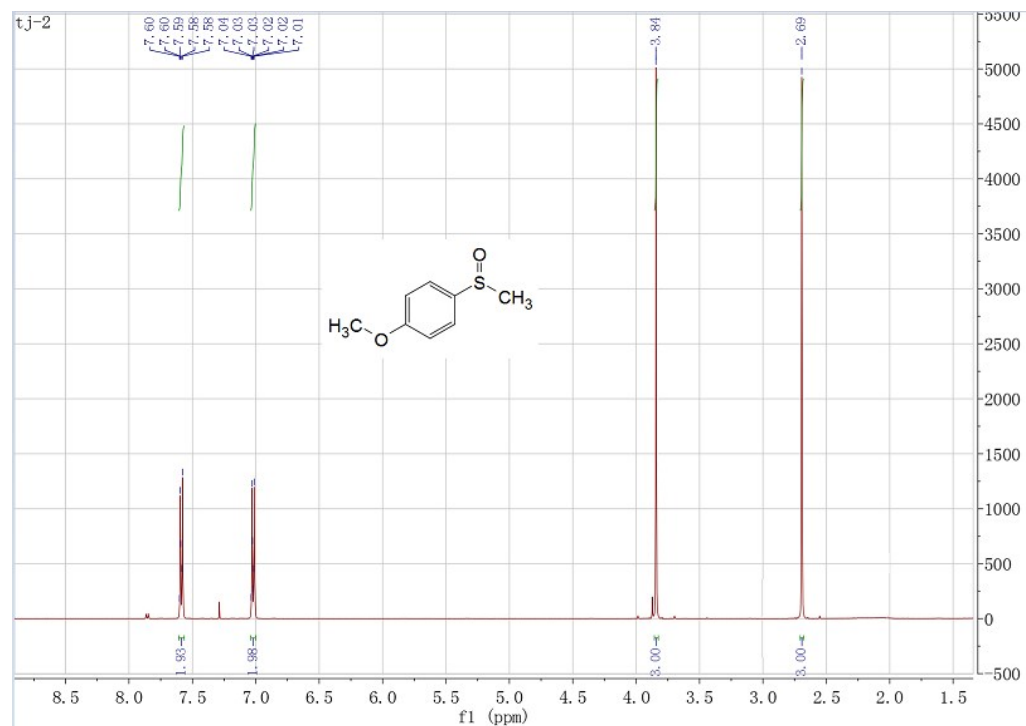
4-Methylphenyl methyl sulfoxide. Colorless oil, purified by flash chromatography on silica gel (ethyl acetate/petroleum ether, v/v = 2:3) (91%). ^1H NMR (500 MHz, CDCl_3) δ (ppm): 7.53-7.49 (m, 2H), 7.30 (d, J = 8.0 Hz, 2H), 2.68 (s, 3H), 2.38 (s, 3H); ^{13}C NMR (126 MHz, CDCl_3) δ (ppm): 142.3, 141.5, 130.0, 129.8, 123.5, 123.3,

43.9, 21.4. Determination of *ee* by HPLC analysis: *n*-hexane/2-PrOH (50:50), 0.5 mL/min, 254 nm, t_r (*S*) = 9.7 min, t_r (*R*) = 16.5 min.



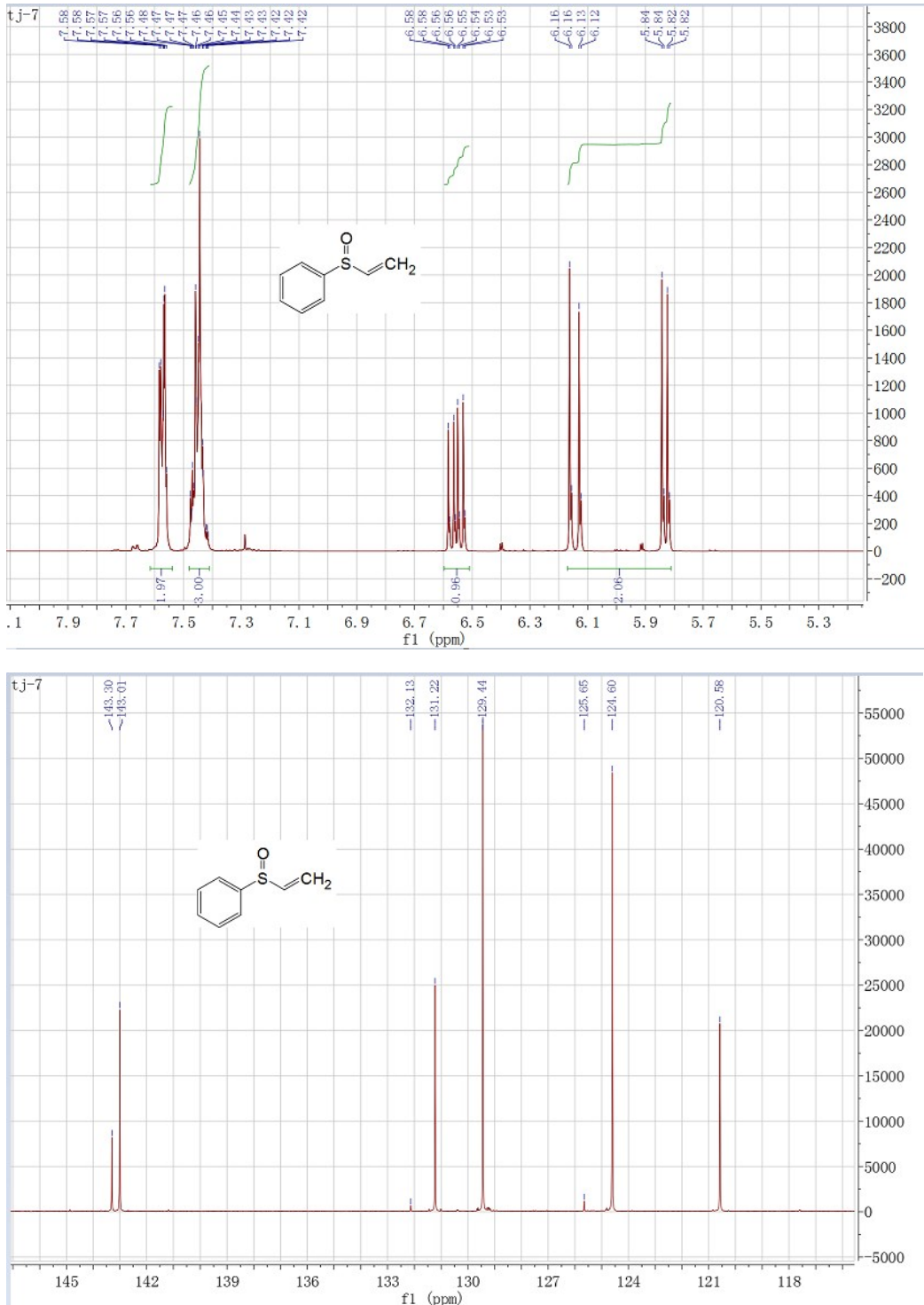
4-Methoxyphenyl methyl sulfoxide. Yellow oil, purified by flash chromatography on silica gel (ethyl acetate/petroleum ether, *v/v* = 2:3) (98%). ^1H NMR (500 MHz, CDCl_3) δ (ppm): 7.61-7.56 (m, 2H), 7.04-7.00 (m, 2H), 3.84 (s, 3H), 2.69 (s, 3H); ^{13}C NMR (126 MHz, CDCl_3) δ (ppm): 162.0, 136.5, 129.5, 125.5, 114.9, 114.5, 55.5,

43.9. Determination of *ee* by HPLC analysis: *n*-hexane/2-PrOH (80:20), 1 mL/min, 254 nm, t_r (*S*) = 12.2 min, t_r (*R*) = 24.6 min.



Vinyl phenyl sulfoxide. Yellow oil, purified by flash chromatography on silica gel (ethyl acetate/petroleum ether, *v/v* = 3:1) (23%). ^1H NMR (500 MHz, CDCl_3) δ (ppm): 7.57 (dt, J = 4.6, 2.7 Hz, 2H), 7.48-7.41 (m, 3H), 6.55 (m, J = 16.5, 9.6, 2.7 Hz, 1H),

6.17-5.81 (m, 2H); ^{13}C NMR (126 MHz, CDCl_3) δ (ppm): 143.3, 143.0, 132.1, 131.2, 129.4, 125.7, 124.6, 120.6. Determination of *ee* by HPLC analysis: *n*-hexane/2-PrOH (90:10), 1 mL/min, 254 nm, t_r (*S*) = 18.8 min, t_r (*R*) = 30.1 min.



Methyl benzyl sulfoxide. Colorless oil, purified by flash chromatography on silica gel (ethyl acetate/petroleum ether, v/v = 1:1) (87%). ^1H NMR (500 MHz, CDCl_3) δ (ppm): 7.43-7.36 (m, 3H), 7.33-7.30 (m, 2H), 4.02 (dd, J = 69.3, 12.8 Hz, 2H), 2.48 (s,

3H); ^{13}C NMR (126 MHz, CDCl_3) δ (ppm): 130.5, 130.0, 129.7, 129.2, 129.0, 128.5, 60.4, 37.3. Determination of *ee* by HPLC analysis: *n*-hexane/2-PrOH (90:10), 1.5 mL/min, 210 nm, t_r (*S*) = 13.7 min, t_r (*R*) = 18.2 min.

